University of Nebraska - Lincoln
DigitalCommons@University of Nebraska - Lincoln

Anthony F. Starace Publications | Research Papers in Physics and Astronomy

October 1984

Photoionization of atomic chlorine above the ^1S threshold

Siamak Shahabi
University of Nebraska - Lincoln

Anthony F. Starace
University of Nebraska-Lincoln, astarace1@unl.edu

T.N. Chang
University of Southern California, Los Angeles, California

Follow this and additional works at: https://digitalcommons.unl.edu/physicsstarace

Part of the Physics Commons

Shahabi , Siamak ; Starace, Anthony F.; and Chang, T.N., "Photoionization of atomic chlorine above the ^1S threshold" (1984). *Anthony F. Starace Publications*. 25.
https://digitalcommons.unl.edu/physicsstarace/25

This Article is brought to you for free and open access by the Research Papers in Physics and Astronomy at DigitalCommons@University of Nebraska - Lincoln. It has been accepted for inclusion in Anthony F. Starace Publications by an authorized administrator of DigitalCommons@University of Nebraska - Lincoln.

Photoionization of atomic chlorine above the ^1S threshold

Siamak Shahabi and Anthony F. Starace
Department of Physics and Astronomy, The University of Nebraska, Lincoln, Nebraska 68588-0111

T. N. Chang
Department of Physics, The University of Southern California, Los Angeles, California 90089-0484
(Received 13 April 1984)

The total photoionization cross section of the $3p$ subshell of atomic chlorine is presented with use of the recently developed open-shell transition-matrix method of Starace and Shahabi. The role of electron correlations is studied by comparison with Hartree-Fock and close-coupling calculations. In contrast to $3p$-subshell photoionization of argon, it is shown that, in chlorine, final-state interchannel interactions are very strong while virtual pair excitations have a weak effect on the shape of the cross section, serving mainly to reduce the discrepancy between length and velocity results. Our results are compared in detail with other theoretical results above the ^1S threshold as well as with experimental relative-intensity measurements at 584 Å. While our results are lower than the others at the ^1S threshold ($\hbar\omega=0.6$ a.u.), at photon energies $\hbar\omega>1$ a.u., our geometric mean cross section is in essentially exact agreement with unrelaxed ionic core results of Brown, Carter, and Kelly and of Fielder and Armstrong.

I. INTRODUCTION

Atomic chlorine has served as a test case for theoretical treatments of electron correlation effects on the photoionization cross section of open-shell atoms.[1–6] One reason[2] for the choice of chlorine is that it is adjacent to argon in the Periodic Table and thus could be compared with known results for argon, which has served as a test case for theories of closed-shell atom photoionization processes.[7] However, the same theoretical methods which produce results in good agreement for photoionization of the $3p$ subshell of argon[7] produce disparate results for the photoionization of the $3p$ subshell of atomic chlorine.[1–6] Experimental data for atomic chlorine photoionization presently exist below the ^1S ionic threshold in the autoionization region[8] and at one energy (584 Å) above.[9] As most theoretical calculations have focused on the region above the ^1S threshold, comparison of the theoretical results with each other is at present the main means for judging their correctness. While all theories find much stronger final-state interactions in chlorine than in argon, the role of virtual pair excitations, which are so important for argon, have not been analyzed in detail for chlorine.

The present paper extends the computational evidence on the photoionization of the $3p$ subshell of atomic chlorine above the ^1S threshold. These results are the first using the recently developed open-shell transition-matrix (OSTM) method,[10] which is a generalization of the transition-matrix method for closed-shell atom photoionization.[11] To demonstrate the role of different kinds of electron correlations, the present results are given in three levels of approximation: Hartree-Fock (HF); close-coupling (CC), including only final-state interchannel interactions; and (OSTM), including, in addition, the effects of virtual electron pair excitations in both initial and final states. The roles of these electron correlations in the photoionization of atomic chlorine are compared and contrasted with those in argon.

Section II presents a brief overview of the OSTM method and its application to the photoionization of chlorine. Section III discusses a number of numerical details of our calculations. Section IV presents our results, their comparison with results for photoionization of argon, and their comparison with other theoretical and experimental results for chlorine. Section V summarizes our conclusions. A more detailed presentation of these results is given elsewhere.[12]

II. THEORY

A. Transition-matrix approach to photoionization

The essential idea of the transition-matrix approach[11] is that in studying a particular reaction or transition process it is unnecessary to consider those electron correlations which do not influence the transition of interest. Rather than study an initial state $\langle i|$ and a final state $|f\rangle$ separately, one studies the outer product $|f\rangle\langle i|$ directly since it is the spatial integration of this outer product with the transition operator which gives the transition-matrix elements of interest. The outer product satisfies the commutation relation

$$[H,\ |f\rangle\langle i|]=\hbar\omega\,|f\rangle\langle i|\ , \tag{1}$$

where H is the exact Hamiltonian operator and $\hbar\omega$ is the transition energy or the energy difference between the initial and final states. The approximations in this method are twofold. The first is the choice of representation of the initial and final states; the second is the choice of interactions to be included in Eq. (1). Since photoionization is induced by the one-electron electric dipole operator, it is convenient to represent the initial and final states as linear

 ©1984 The American Physical Society

combinations of one-electron orbitals. Generally it is most convenient to represent the spectator electrons in the photoionization transition by the atomic HF orbital wave functions. The correlated initial and final wave functions for the electron making the transition, however, are defined by coupled differential equations derived, firstly, by integrating Eq. (1) over all coordinates except the radial coordinate of the transition electron, and secondly, by defining those types of electron correlation in the resulting equations which are to be kept.

The transition-matrix approach was first formulated algebraically for closed-shell atom photoionization processes.[11] The ^1S symmetry of the atomic ground state greatly simplified the algebraic formulation. While the final state was represented by configurations containing only a single electron excited out of the ground configuration, the initial state was represented not only by a closed-shell configuration but also by additional configurations having pairs of electrons excited out of the closed-shell configuration. In solving the differential equations derived from Eq. (1), only those electron correlations constituting the well-known random-phase approximation[13] (RPA) were kept.

The generalization[10] of the transition-matrix method to treat open-shell atom photoionization processes was formulated using graphical methods for carrying out the more involved angular-momentum algebra. As in the closed-shell atom case, the most complicated electron correlations are those involving the configurations having a pair of electrons excited out of the ground configuration. A key contribution of the graphical approach is in showing that the RPA-equivalent, closed-shell atom transition-matrix equations may be obtained from the following approximation to the exact transition-matrix equations (given the form of the initial and final state described above): the exact interaction of the excited pairs of electrons in the ground state with the ionic-core electrons is approximated by an interaction in which *the excited electrons exchange zero orbital and spin angular momenta with the ionic core.* This definition of the RPA-equivalent, closed-shell atom transition-matrix equations is actually not dependent on having a closed-shell (i.e., ^1S) ground state. It therefore serves as a convenient way to define an RPA-type treatment of open-shell atom photoionization processes. Since, however, several different RPA treatments for open-shell systems have already been developed,[3,14–16] we distinguish our treatment here from the others by referring to it as the OSTM method.[10]

B. Application to atomic chlorine

Since the transition-matrix method[11] and its open-shell atom generalization[10] have been presented in detail elsewhere, and since the key ideas of these theories and their relationships have been reviewed recently as well,[17] we present here only those details of the theory specific to photoionization of atomic chlorine. We are concerned with the following photoionization process:

$$\mathrm{Cl}[3p^5(^2P)]+\gamma\rightarrow \mathrm{Cl}^+[3p^4(\tilde{L}\tilde{S})]+e^- , \tag{2}$$

where $\tilde{L}$ and $\tilde{S}$ denote the orbital and spin quantum numbers of the ion, which may have the values ^3P, ^1D, and ^1S. The final and initial states are assumed to have the following forms:

$$|f^{\alpha'}\rangle \equiv \sum_{\tilde{L},\tilde{S},l} |3p^4(\tilde{L}\tilde{S})\psi^{\alpha'}_{(\tilde{L}\tilde{S})l}\,2L\rangle , \tag{3a}$$

$$\langle i| \equiv \langle 3p^5\,{}^2P| + \sum_{\substack{\bar{L},\bar{S},l_\phi\\ L_P,S_P}} b(\bar{L}\bar{S},L_PS_P,l_\phi) \times \langle 3p^3(\bar{L}\bar{S})\phi_a\phi_b(L_PS_P)^2P| . \tag{3b}$$

In Eq. (3a), ^2L denotes the term levels of the final state, which may have values ^2D, ^2P, and ^2S, α denotes a particular final-state channel defined by the ionic, photoelectron, and system angular-momentum quantum numbers $(\tilde{L}\tilde{S})l(^2L)$, and $\psi^{\alpha'}_{(\tilde{L}\tilde{S})l}(r)\equiv\psi^{\alpha'}_{\alpha}(r)$ denotes the radial one-electron wave function in the αth channel for the final state in which the photoelectron is asymptotically in the α' channel. The kinetic energy ϵ_α of the photoelectron used to compute each of the radial wave functions $\psi^{\alpha'}_{\alpha}(r)$ is fixed by the photon energy E_γ and by the binding energies I_α for each channel: $\epsilon_\alpha=E_\gamma-I_\alpha$.

In Eq. (3b) the initial state is represented by the main configuration $3p^5$ plus a sum over configurations having a pair of electrons, each with orbital angular momentum $l_\phi=0$ or 2, excited out of the main configuration. The excited electrons are represented by bounded radial wave functions $\phi_a(r)$ and $\phi_b(r)$. Because of the sums over the term levels $\bar{L}\bar{S}$ of the $3p^3$ core as well as over the term levels L_PS_P of the excited electron pair, the representation in Eq. (3b) appears to be quite complex. Actually, however, since the electric dipole transition operator is a one-electron operator, only certain limited *linear combinations* of the excited electron radial functions $\phi_a(r)$ and $\phi_b(r)$ are needed for calculating photoionization cross sections.[10,11] These linear combinations are different for each final-state channel α' and are denoted by $\phi^{\alpha'}_{(\Lambda\Sigma)l_\phi}(r)$, where the quantum numbers Λ and Σ may assume all integer values consistent with the triangular relations

$$|L-1|\leqq\Lambda\leqq L+1 , \tag{4a}$$

$$|l_\phi-1|\leqq\Lambda\leqq l_\phi+1 , \tag{4b}$$

$$0\leqq\Sigma\leqq 1 . \tag{4c}$$

The explicit but complex analytical expression for each of the one-electron functions $\phi^{\alpha'}_{(\Lambda\Sigma)l_\phi}(r)$, which we refer to here as the ground-state correlation functions, is given in Eq. (13b) of Ref. 10.

Substituting the forms for the final and initial states in Eq. (3) into the equation of motion in Eq. (1), integrating the latter equation over all electron coordinates except the radial coordinate of the last electron, and carrying out extensive further reductions, one obtains a set of coupled differential equations for the radial wave functions $\psi^{\alpha'}_{(\tilde{L}\tilde{S})l}(r)$ and $\phi^{\alpha'}_{(\Lambda\Sigma)l_\phi}(r)$. The full list of coupled radial functions is shown in Table I. For example, for each of the four ^2D final states α' there are four final-state radial functions $\psi^{\alpha'}_{(\tilde{L}\tilde{S})l}(r)$ and eight ground-state correlation

TABLE I. Explicit list of coupled radial wave functions in the $3p$-subshell photoionization of atomic chlorine.

Final state (^2L)	$\psi_{(\tilde{L}\tilde{S})l(L_f S_f)}$	$\phi_{(\Lambda\Sigma)l_\phi}$	$\mathcal{N}$ is the number of unknown functions as well as the number of equations to be solved simultaneously. $\mathcal{N}$
^2S	$\psi_{(^1S)s}$	$\phi_{(10)s}, \phi_{(11)s}$	6
	$\psi_{(^1D)d}$	$\phi_{(10)d}, \phi_{(11)d}$	
^2P	$\psi_{(^3P)s}$	$\phi_{(10)s}, \phi_{(11)s}$	9
	$\psi_{(^3P)d}$	$\phi_{(10)d}, \phi_{(11)d}$	
	$\psi_{(^1D)d}$	$\phi_{(20)d}, \phi_{(21)d}$	
^2D	$\psi_{(^1S)d}$	$\phi_{(10)s}, \phi_{(11)s}$	12
	$\psi_{(^3P)d}$	$\phi_{(10)d}, \phi_{(11)d}$	
	$\psi_{(^1D)s}$	$\phi_{(20)d}, \phi_{(21)d}$	
	$\psi_{(^1D)d}$	$\phi_{(30)d}, \phi_{(31)d}$	

functions, $\phi^{\alpha'}_{(\Lambda\Sigma)l_\phi}(r)$, giving a system of twelve coupled radial differential equations to be solved at each photon energy. Analytic expressions for these differential equations are given in Eqs. (14) and (15) of Ref. 10; numerical values for the angular-momentum coefficients in these equations for the case of atomic chlorine are given in Appendix F of Ref. 12. Note that when our correlation functions $\phi^{\alpha'}_{(\Lambda\Sigma)l_\phi}(r)$ are set equal to zero, our coupled differential equations for the radial functions $\psi^{\alpha'}_{(\tilde{L}\tilde{S})l}(r)$ become identical to the usual close-coupling (CC) equations.[18] If, in addition, the coupling terms between the final-state channels α are dropped, each of the radial functions $\psi^{\alpha'}_{\alpha}(r)$ with $\alpha'=\alpha$ becomes the HF function computed in the $V^{N-1}(LS)$ potential[19] appropriate for the channel α.

In this paper our results for the $3p$-subshell photoionization cross section of atomic chlorine obtained by solving the full set of coupled differential equations indicated in Table I are referred to as our OSTM results. They are compared with our results in the simpler CC and HF approximations. Due to the large amount of computer time required to solve up to twelve coupled differential equations for numerous photon energies, we have not investigated the influence on the chlorine $3p$-subshell cross section of the following three effects: (1) The interchannel interaction of the chlorine $3p$-subshell channels with the chlorine $3s$-subshell channels, (2) the interchannel interaction of the nine chlorine $3p$-subshell channels listed in Table I with the tenth allowed channel, $Cl^+(^1D)\epsilon g(^2D)$, which is the only one not permitted in an independent-particle approximation, and (3) relaxation of the ionic core during the photoionization process. The possible influence of the first and third of these effects is discussed in Sec. IV below.

III. NUMERICAL DETAILS

A. Boundary conditions

At the origin the correlation functions and the final-state radial wave functions satisfy the conditions

$$\phi^{\alpha'}_{(\Lambda\Sigma)l_\phi}(r) \to r^{l_\phi+1} \text{ as } r\to 0 , \tag{5a}$$

$$\psi^{\alpha'}_{(\tilde{L}\tilde{S})l}(r) \to r^{l+1} \text{ as } r\to 0 . \tag{5b}$$

At infinity the correlation function is bounded and the final-state radial wave function is energy normalized:

$$\phi^{\alpha'}_{(\Lambda\Sigma)l_\phi}(r) \to 0 \text{ as } r\to\infty , \tag{6a}$$

$$\psi^{\alpha'}_{\alpha}(r) \to \left[\frac{2}{\pi k_\alpha}\right]^{1/2} [\sin(\theta_\alpha+\delta^{\rm HF}_\alpha)\delta_{\alpha'\alpha} + \cos(\theta_\alpha+\delta^{\rm HF}_\alpha)R_{\alpha'\alpha}] \quad \text{as } r\to\infty . \tag{6b}$$

In Eq. (6b), $\epsilon_\alpha \equiv k_\alpha^2/2$ is the photoelectron's kinetic energy in the αth channel, the argument θ_α is defined by

$$\theta_\alpha(k_\alpha,r) \equiv k_\alpha r - \tfrac{1}{2}\pi l + \frac{1}{k_\alpha}\ln(2k_\alpha r) + \arg\Gamma(l+1-i/k_\alpha) , \tag{7}$$

$\delta^{\rm HF}_\alpha$ is the HF phase shift in channel α at photoelectron kinetic energy ϵ_α, and $R_{\alpha'\alpha}$ is the reaction matrix with respect to a HF reference basis. The reaction matrix[20] R is equal to the K matrix[21,22] of scattering theory multiplied by $-\pi$; the on-the-energy-shell parts of the R and K matrices, denoted by curly brackets, are related to the S matrix as follows:

$$S=(1+i\{R\})(1-i\{R\})^{-1}=(1-i\pi\{K\})(1+i\pi\{K\})^{-1} . \tag{8}$$

The Coulomb phase in Eq. (7) as well as the r-dependent Coulomb amplitude, applicable at finite r, for the radial functions in Eq. (6b) were computed using the procedure of Martins.[23]

The continuous wave functions normalized using the standing-wave representation in Eq. (6b) are convenient for numerical purposes as they are real. The final-state wave function in a multichannel photoionization process, however, must satisfy incoming-wave boundary conditions.[24] The transformation from standing-wave to incoming-wave normalization is carried out on the dipole matrix elements calculated with use of the real wave functions normalized as in Eq. (6). This transformation is given in Sec. III C.

B. Solution of the differential equations

1. Orthogonality constraints

Accurate numerical results require the orthogonality of final-state wave functions to ground-state orbitals having the same orbital angular momentum l. For photoionization of the $3p$ subshell of chlorine, therefore, the continuum s electrons must be made orthogonal to the $1s$, $2s$, and $3s$ bound orbitals. This will be accomplished if both bound and continuum s orbitals are computed in the same Hermitian potential. As our bound s-electrons are computed in the appropriate HF potential for the atom $V_{\rm atom}$, and as we wish our continuum s electrons to be computed

in the appropriate $V^{N-1}(LS)$ potential[19] for the ion, a single Hermitian potential V for both bound and continuum states must of necessity be constructed using projection operators as follows:[25–27]

$$V = V_{\text{atom}} + (1-P)\Delta V(1-P) , \tag{9a}$$

where

$$P \equiv \sum_{n=1}^{3} |ns\rangle\langle ns| \tag{9b}$$

and

$$\Delta V \equiv V^{N-1}(LS) - V_{\text{atom}} . \tag{9c}$$

The projection operator P in Eq. (9b) is defined by a sum over all three bound HF one-electron s orbitals in the atom. The action of the operator V on bound and continuum one-electron s orbitals $|ns\rangle$ and $|\epsilon s\rangle$ is

$$V|ns\rangle = V_{\text{atom}}|ns\rangle , \tag{10a}$$

$$V|\epsilon s\rangle = V^{N-1}(LS)|\epsilon s\rangle - \sum_{n=1}^{3} |ns\rangle\langle ns|\Delta V|\epsilon s\rangle . \tag{10b}$$

The coefficients of the bound orbitals $|ns\rangle$ in Eq. (10b), $\langle ns|\Delta V|\epsilon s\rangle$, are the Lagrangian parameters needed to ensure orthogonality of $|\epsilon s\rangle$ and $|ns\rangle$. A similar procedure is used to obtain the Lagrangian parameters for ensuring orthogonality of the s-type correlation functions to the $1s$, $2s$, and $3s$ orbitals. Expressions in terms of Slater integrals for the Lagrangian parameters used in the present calculations are given in Table III of Ref. 12.

2. *Iterative procedure*

The coupled differential equations in our calculation are second order, linear, and inhomogeneous. As the first derivative is absent, we use a Numerov outward integration procedure and solve our equations iteratively. The first step is to ignore all coupling terms in the equations and thereby obtain the continuum HF wave functions. These are then used to evaluate the interchannel coupling matrix elements. The solutions of the coupled continuum equations are the CC wave functions. Finally the CC wave functions are used to compute the coupling matrix elements which serve as source terms for the bound correlation functions. Solution of our fully coupled set of equations produces the OSTM wave functions $\psi_\alpha^{\alpha'}(r)$ and $\phi_{(\Lambda\Sigma)l_\phi}^{\alpha'}(r)$. In solving the coupled differential equations for channel α iteratively, we stop iterating when the phase shift of the radial function $\psi_\alpha^\alpha(r)$ has converged. These numerical procedures are similar to those described elsewhere[28–30] for solving the closed-shell atom transition-matrix equations.

3. *Binding energies*

The binding energies used in solving the differential equations can have a significant influence on the photoionization cross sections near threshold. The transition-matrix equations imply the use of the HF binding energy for the $3p$ subshell of chlorine: $I_{3p}^{\text{HF}} = 0.506\,52$ a.u. Other interactions are needed to reproduce the fine-structure average of the experimental binding energies[31] for each ionic term level:

$$I(^3P) = 0.4768 \text{ a.u.} , \tag{11a}$$

$$I(^1D) = 0.5283 \text{ a.u.} , \tag{11b}$$

$$I(^1S) = 0.6022 \text{ a.u.} \tag{11c}$$

We have solved each coupled set of differential equations twice: once using the HF binding energy and once using the experimental binding energies.

4. *Numerical tests*

Several tests of our numerical procedures have been carried out. Firstly, the HF part of our code produced results in essentially exact (i.e., four-digit) agreement with those of the continuum HF code of Bates.[32] Secondly, our coupled channel code was tested by reproducing exactly the transition-matrix results of Chang[28] for argon $3p$-subshell photoionization. Thirdly, the symmetry of our R-matrix elements in our chlorine calculations was checked. We found that the R-matrix elements for interacting d channels were symmetric to three digits, while those for interacting s and d channels were symmetric to only two digits. Excluding the s channels entirely, however, did not significantly affect the cross-section results, but it did improve the symmetry of the R-matrix elements between d channels to four digits. Because of the weak effect of the s channels on the cross sections, we did not search any further for the cause of the very slight asymmetry in the R-matrix elements coupling s and d channels. Fourthly, doubling our mesh size had an insignificant effect on our results (i.e., changes were in the seventh digit).

C. Cross-section formulas

The dipole matrix element for transition to the final-state channel α' in terms of the standing-wave—normalized wave functions in Eq. (6b) is given by

$$D_{\alpha'} \equiv \sum_{\tilde{L},\tilde{S},l} G(\tilde{L},\tilde{S},l)\langle 3p||r||\psi_{(\tilde{L}\tilde{S})l}^{\alpha'}\rangle + \sum_{\Lambda,\Sigma,l_\phi} H(\Lambda,\Sigma,l_\phi)\langle \phi_{(\Lambda\Sigma)l_\phi}^{\alpha'}||r||3p\rangle . \tag{12}$$

Here the reduced matrix element for the length form of the electric dipole operator is given by

$$\langle n_l l_1||r||n_2 l_2\rangle \equiv (-1)^{l_1-l_>} l_>^{1/2} \int_0^\infty P_{n_1 l_1}(r) r P_{n_2 l_2}(r) dr , \tag{13a}$$

where

$$l_> \equiv \max(l_1, l_2) . \tag{13b}$$

Analytic expressions for the G and H coefficients for an arbitrary atom are given in Eqs. (18b) and (18c) of Ref. 10. Numerical values for these coefficients for the case of chlorine $3p$-subshell photoionization are given in Appendix H of Ref. 12. The symbol "$3p$" in the reduced matrix elements in Eq. (12) refers in our calculations to the HF

$3p$ radial wave function for the atomic ground state of chlorine. Velocity-form expressions for the electric dipole matrix elements $D_{\alpha'}$ are similar to Eq. (12) but employ the reduced matrix elements for the gradient operator.[33]

To compute the partial cross sections for photoionization to a particular final-state channel the final-state wave function must satisfy incoming-wave boundary conditions.[24] The transformation from standing-wave to incoming-wave normalization is carried out on the dipole matrix elements in Eq. (12) as follows:[20,22]

$$D_{\alpha'}^{(-)} \equiv \sum_{\alpha} D_{\alpha}[(\mathbb{1}+i\{R\})^{-1}_{\alpha\alpha'}]\exp(-i\delta_{\alpha'}^{\mathrm{HF}}) . \tag{14}$$

Here the minus superscript on the transformed dipole matrix element denotes the use of an incoming-wave—normalized final state. The exponential factor involving the HF phase shift in channel α' is necessary since our R matrix is determined with respect to a HF basis.

The partial photoionization cross section to the channel α' is given by[34]

$$\sigma_{\alpha} = \frac{4\pi^2}{3c}\omega\frac{1}{2L_0+1}|D_{\alpha}^{(-)}|^2 . \tag{15}$$

Here L_0 is the term level for the ground state of chlorine, i.e., $L_0=1$, and ω is the photon energy in atomic units. Substitution of Eq. (14) in Eq. (15) gives the following explicitly real expression for the partial cross section in terms of the real standing-wave—normalized dipole matrix elements and the real R-matrix elements:

$$\sigma_{\alpha} = \frac{4\pi^2}{3c}\frac{\omega}{(2L_0+1)}\left[\sum_{\alpha'\alpha''} D_{\alpha'}[(1+\{R\}^2)^{-1}]_{\alpha'\alpha}[(1+\{R\}^2)^{-1}]_{\alpha\alpha''}D_{\alpha''} + \sum_{\alpha',\alpha''} D_{\alpha'}[(1+\{R\}^2)^{-1}\{R\}]_{\alpha'\alpha}[\{R\}(1+\{R\}^2)^{-1}]_{\alpha\alpha''}D_{\alpha''}\right] . \tag{16}$$

In both Eq. (14) and (16), $\{R\}$ denotes the on-the-energy-shell part of the R matrix for total energy ω relative to the ground state of chlorine.

IV. RESULTS

A. Total cross section

Our calculations of the total photoionization cross section for the $3p$ subshell of atomic chlorine above the ^1S ionic threshold are shown in Fig. 1. Length and velocity formula results in the HF, CC, and OSTM approximations are shown. All of these results employ experimental binding energies (cf. Eq. 11). At threshold the independent-channel HF length and velocity results are higher than the CC and OSTM results by about a factor of 2. For higher photon energies the HF cross sections decrease monotonically. The coupling of final-state channels in the CC and OSTM calculations leads to a drastic change in the energy dependence of the corresponding cross sections. The CC and OSTM results peak above threshold at a photon energy of about 0.78 a.u. rather than decreasing monotonically. The difference between the length and velocity cross sections is made worse in the CC approximation as compared to the HF approximation. This difference in the CC results is diminished in the OSTM approximation but is not eliminated.

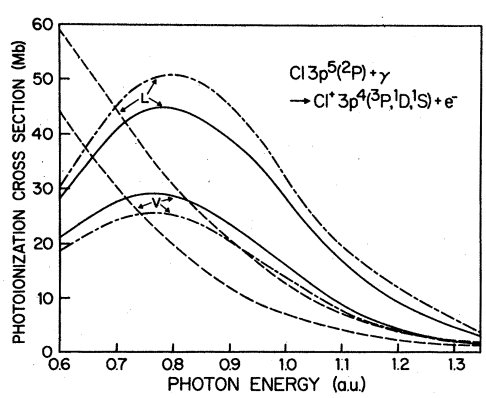

FIG. 1. Total photoionization cross section for the $3p$ subshell of atomic chlorine above the ^1S ionic threshold calculated using experimental binding energies in HF (dashed curves), CC (dot-dash curves), and OSTM (solid-line curves) approximations. L and V denote cross sections obtained with dipole length and velocity formulas.

B. Comparison of Ar and Cl

In order to compare the relative importance of different kinds of electron correlations on the $3p$-subshell photoionization cross sections of the closed- and open-shell atoms Ar and Cl, consider the results shown in Figs. 2 and 3.

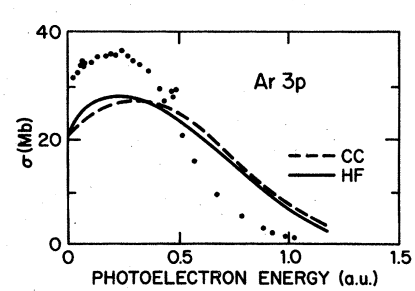

FIG. 2. Photoionization cross-section results for the $3p$ subshell of argon. HF: geometric mean of the theoretical Hartree-Fock-equivalent, length and velocity K-matrix results of Starace (Ref. 36). CC: geometric mean of the theoretical close-coupling length and velocity results of Lipsky and Cooper (Ref. 37). Solid circles: experimental results of Samson (Ref. 38).

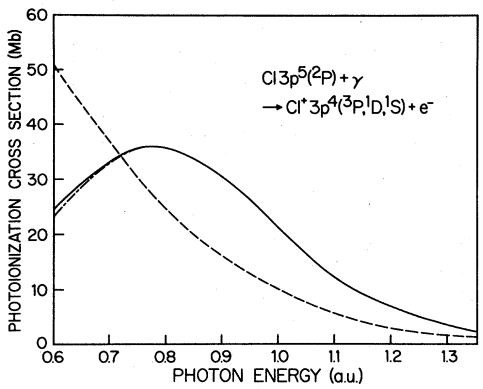

FIG. 3. Total photoionization cross sections for the $3p$ subshell of atomic chlorine above the ^1S ionic threshold calculated using experimental binding energies in HF (dashed curve), CC (dot-dash curve), and OSTM (solid-line curve) approximations. The geometric means of the length and velocity results in Fig. 1 are shown.

To focus attention on the energy dependence of the cross sections rather than on the discrepancy between length and velocity results, the theoretical results in these figures are given using the geometric mean[35] of the length and velocity cross-section results. In Fig. 2 the theoretical results labeled HF are the geometric-mean results of an intrachannel K-matrix calculation,[36] which is equivalent to a HF calculation. The CC results[37] treat interchannel interactions between the two final-state channels that are allowed in LS coupling: $Ar^+\ 3p^5\epsilon d(^1P)$ and $Ar^+\ 3p^5\epsilon s(^1P)$. The solid circles are experimental results,[38] but serve as a proxy for the closed-shell atom transition-matrix results[39] as well as for several other RPA-equivalent theoretical results.[7] The near equivalence of the geometric-mean HF and CC curves in Fig. 2 implies that the final-state interchannel interactions are weak, most probably because only a single d channel is permitted in LS coupling. Figure 1 of Ref. 36 shows that the discrepancy between the length and velocity curves is somewhat worse in the CC approximation as compared to the HF calculation, just as was found for Cl in our Fig. 1.

The transition matrix[39] and other RPA-equivalent methods,[7] which take into account the effect of virtual electron pairs excited out of the ground configuration, produce a drastically different energy dependence for the argon $3p$-subshell photoionization cross section, raising it at threshold and lowering it at higher energies, in the process bringing theory and experiment into agreement. Furthermore, inclusion of the correlations involving virtually excited electron pairs brings the length and velocity results into very close agreement.[7,39]

In contrast, Fig. 3 shows a much different role in chlorine for the same kinds of electron correlations. This figure shows the geometric mean of the length and velocity results in Fig. 1. Here one sees that the CC results are drastically changed from the HF results, implying strong final-state interchannel interactions, primarily those between final-state d channels. The geometric-mean CC and OSTM results in Fig. 3 are nearly identical, implying an insignificant role for correlations involving virtual electron pairs excited out of the ground configuration. Their sole role seems to be to reduce the discrepancy between the CC approximation length and velocity results, as shown in Fig. 1. This reduced role for RPA-type ground-state correlations on the $3p$-subshell photoionization cross sections of Cl as compared to Ar confirms earlier results of Starace and Armstrong.[2]

C. Comparison with other theoretical results

Our geometric-mean results for the photoionization cross section of atomic chlorine above the ^1S threshold are compared with the geometric-mean results of other calculations including at least final-state interchannel coupling in Fig. 4. We present the geometric-mean results because it makes the presentation of the eight different calculations shown more tractable than would the presentation of length and velocity results for each calculation. We have computed the geometric mean simply as the square root of the product of the length and velocity results for each curve. We believe this presents these results accurately for the following reasons. Firstly, the total geometric-mean cross section *should* be calculated as the sum of the geometric-mean partial cross sections for each of the final-state channels considered and *not* as the square root of the product of the total length and total velocity cross sections. In our calculations, however, the difference between the correct computation method and the much simpler approximate method is 0.25% at the ^1S threshold and 0.44% at 584 Å. Differences of this magnitude are barely resolvable on the scale of our Fig. 4 and are thus of no consequence. Secondly, as shown in Table II, the length-velocity differences at the ^1S threshold of five out of six of the calculations, other than our own, shown in Fig. 4 are less than 12%. These small differences imply

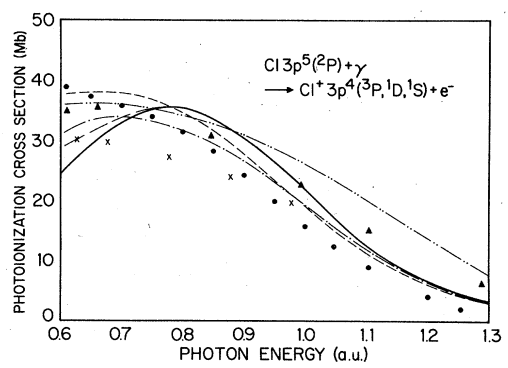

FIG. 4. Theoretical geometric-mean total photoionization cross sections for the $3p$ subshell of atomic chlorine above the ^1S ionization threshold. *Solid line:* present OSTM results using experimental binding energies. *Long dashed line:* present OSTM results using HF binding energy. *Crosses:* CC results of Conneely, Ref. 1(a) (Table XX). *Solid circles:* RPA results of Cherepkov and Chernysheva, Ref. 3(b) (Fig. 7). *Short dashed line:* unrelaxed-core MBPT results of Brown, Carter, and Kelly, Ref. 4(b) (Table III). *Solid triangles:* relaxed-core MBPT results, Ref. 4(b) (Table III). *Dash—double-dot line:* R-matrix (Case II) results of Lamoureux and Combet-Farnoux, Ref. 5 (Fig. 2). *Dash-dot line:* correlated final-state MCHF results of Fielder and Armstrong, Ref. 6(b) (Table LIV).

TABLE II. Main features of the theoretical calculations shown in Fig. 4.

Feature	Theoretical calculations: Conneely[a] (CC)	Cherepkov and Chernysheva[b] (RPA)	Present results (OSTM)	Fielder and Armstrong[c] (MCHF)	Brown, Carter, and Kelly[d] (MBPT)	Lamoureux and Combet-Farnoux[e] (R matrix)
Final-state interchannel interactions?	Yes	Yes[f]	Yes	Yes[g]	Yes	Yes
Pair excitations from $3p$ subshell?	No	Yes	Yes	Yes	Yes	Yes
Excitations from $3s$ subshell?	No	No	No	Yes	Yes	Yes
Relaxed (R) or unrelaxed (U) ion core?	R	U	U	U	U,R	R
Length-velocity disagreement[h] at ^1S threshold?	+60%	"identical to within precision of the calculation"[b]	+30%	−12%	+9% (U) +5% (R)	+9%

[a]Ref. 1.
[b]Ref. 3.
[c]Ref. 6.
[d]Ref. 4.
[e]Ref. 5.
[f]Interaction between two channels treated exactly; interactions with additional channels treated approximately.
[g]Interaction among up to three channels treated exactly; interactions of $3p \rightarrow d$ channels with $3p \rightarrow s$ channels neglected in some cases.
[h]Defined by $100\,(\sigma_L - \sigma_V)/\sigma_{GM}$ where σ_L and σ_V are the total length and velocity photoionization cross sections and where σ_{GM} is the geometric mean of these cross sections.

that for the other calculations as well, the discrepancy between the correct and our approximate method of computing geometric-mean total cross sections should be minimal.

The key similarities and differences of each of the theoretical calculations shown in Fig. 4 are indicated in Table II. Both the kinds of electron correlations included in each calculation as well as certain features and limitations of the numerical procedures are indicated. It should be emphasized that Table II serves here only to distinguish the numerous theoretical results in very general terms; it does not and is not meant to characterize them precisely.

The broad similarity of all the results shown in Fig. 4 may be explained (with reference to Table II) by the fact that all calculations include the strong, final-state interchannel interactions. The major effect of additional electron correlations seems to be to reduce the discrepancy between the length and velocity results. As shown in Table II, this discrepancy at the ^1S threshold is 60% in the CC calculations of Conneely.[1] It is reduced to 30% in our OSTM results when virtual pair excitations from the $3p$ subshell are included. It is reduced to about $\pm 10\%$ in the multiconfigurational Hartree-Fock (MCHF),[6] many-body perturbation theory (MBPT),[4] and R-matrix[5] calculations when, in addition, configurations having one or two electrons excited out of the $3s$ subshell are included. Note in particular the minus sign for the MCHF calculation. It indicates that the correlations included bring down the length total cross section and bring up the velocity total cross sections so much that they overshoot, i.e., the velocity cross section is greater than the length cross section. The R-matrix results[5] also confirm the effect of $3p$-subshell and $3s$-subshell excitations on reducing the discrepancy between the length and velocity cross-section results. The R-matrix[5] Case-I calculations (not shown) include only minimal configuration mixing and have a length-velocity discrepancy of 25%; the Case-II calculations (shown) have extensive configuration mixing and have a length-velocity discrepancy of only 9%.

Note that the length-velocity disagreement for most of the results shown in Fig. 4 is much less than the disagreement between the different curves at the ^1S threshold and at high energy. At the ^1S threshold our OSTM results using experimental binding energies give the lowest cross section; our results also rise the most steeply with increasing photon energy. Our results using the HF binding energy are 20% higher at threshold, but become identical to those using the experimental binding energies at a photon energy of 0.78 a.u. Thus the choice of binding energy affects the calculated results only at and just above the ^1S threshold. Both the MCHF[6] and the relaxed-core MBPT[4] results are rising at threshold. The R-matrix,[5] the unrelaxed-core MBPT,[4] and the CC[1] results are fairly flat

at threshold. In contrast, the RPA[3] results are decreasing at threshold.

At photon energies above 1 a.u. our results are in virtually exact agreement with the unrelaxed-core MBPT[4] and MCHF[6] results. The RPA[3] results are about 2 Mb lower; a possible reason for this may be the approximate treatment of interchannel interactions between $3p \rightarrow \epsilon d$ channels in this calculation. The R-matrix[5] and, to a lesser extent, the relaxed-core MBPT[4] results are substantially higher. The results of Brown *et al.*[4] indicate that part of the discrepancy of the R-matrix results from the other calculations is due to the use of a relaxed ionic core. Comparison of the two results of Brown *et al.*[4] shown in Fig. 4 shows that substitution of relaxed-core orbitals for unrelaxed ones tends to lower the total cross section at threshold and to raise it at higher energies. Of course, neither the use of unrelaxed- nor of relaxed-core orbitals is a correct description of ionic relaxation effects on the photoionization process. One can say, however, that the use of relaxed-core orbitals is more nearly correct at threshold, when the photoelectron is escaping slowly, and that the use of unrelaxed-core orbitals is more nearly correct at high photon energies, when the photoelectron is escaping rapidly.

D. Comparison with experimental data

We do not have results to compare with the detailed relative experimental cross sections[8] in the autoionization region below the ^1S threshold. We are able to compare with the relative experimental photoelectron intensity measurements of Kimura, Yamazaki, and Achiba[9] at 584 Å. We caution, however, that since the experimental relative-intensity measurements were made at 90° with respect to the photon beam, they must be corrected for photoelectron angular distribution effects in order to make them comparable to theoretical partial cross-section branching ratios. Having made this caveat, we nevertheless compare the *uncorrected* experimental results with selected theoretical results in Table III.

As none of the theoretical calculations agree with both of the uncorrected experimental results, it is of interest to estimate the magnitude of the corrected experimental results. The necessary correction is given by Samson and Gardner.[40] In order to make the needed correction one needs to know the photoelectron asymmetry parameter values β for each of the three ionic term levels of chlorine. These have been calculated by Fielder and Armstrong,[6] although there is considerable uncertainty between their length and velocity results. Fortunately the correction formulas are not sensitive to small changes in the β values. Thus using the following rough estimates for the β parameters, $\beta(^3P)=0.66$, $\beta(^1D)=0.31$, and $\beta(^1S)=0.47$, we find that the experimental ^1D relative measurement should be increased by approximately 8% and that for ^1S should be increased by approximately 4%. We have not put the corrections in Table III as we do not wish our very approximate estimates to be quoted as "the" experimental values. In particular, none of the theoretical results agrees with both of the experimental values even after correction. This exercise thus emphasizes the need for experimental results over a wide energy range.

V. CONCLUSIONS

We have presented Hartree-Fock (HF), close-coupling (CC), and open-shell transition-matrix (OSTM) results for the total photoionization cross section of the $3p$ subshell of atomic chlorine above the ^1S ionization threshold. Our results indicate that final-state interchannel interactions are the dominant electron correlations. They drastically alter the independent-electron HF results. However, the influence of virtually excited pairs of electrons out of the $3p$ subshell is weak. It has no effect on the geometric-mean OSTM cross section *vis-à-vis* the geometric-mean CC cross section; its main role seems to be to reduce the large discrepancy between the length and velocity cross section in the CC approximation. This behavior is very different from that in $3p$-subshell argon photoionization where virtual pair excitations have a major effect on the

TABLE III. Theoretical length (velocity) values for the Cl^+ $3p^4(^1D)$ and Cl^+ $3p^4(^1S)$ partial photoionization cross sections, relative to that for Cl^+ $3p^4(^3P)$ (normalized to the value 1.5), compared with experimental relative-intensity measurements (obtained at 90° to the photon beam) at the photon energy 584.33 Å (0.78 a.u.).

Method	^3P	^1D	^1S
HF (unrelaxed)[a]	1.5 (1.5)	0.70 (0.83)	0.18 (0.20)
HF (relaxed)[a]	1.5 (1.5)	0.45 (0.58)	0.11 (0.13)
MBPT (unrelaxed)[a]	1.5 (1.5)	0.74 (0.79)	0.13 (0.14)
MBPT (relaxed)[a]	1.5 (1.5)	0.68 (0.72)	0.11 (0.12)
MCHF[b]	1.5 (1.5)	0.78 (0.83)	0.19 (0.19)
OSTM[c]	1.5 (1.5)	0.77 (0.87)	0.11 (0.10)
OSTM[d]	1.5 (1.5)	1.01 (1.10)	0.20 (0.17)
Experiment[e]	1.5	0.81	0.16

[a]E. R. Brown, S. L. Carter, and H. P. Kelly, Ref. 4(b) (Table V).
[b]W. R. Fielder and L. Armstrong, Jr., Ref. 6(a) (Table VI).
[c]Present results using HF binding energies.
[d]Present results using experimental binding energies.
[e]K. Kimura, T. Yamazaki, and Y. Achiba, Ref. 9. These relative-intensity measurements require correction for photoelectron angular distribution effects in order to be comparable to theoretical results. See discussion in text.

calculated cross sections.

In comparison with other theoretical results above the ^1S ionization threshold, our results are the lowest at the ^1S threshold and rise rapidly to a maximum at about 0.78-a.u. photon energy. Above 1.0-a.u. photon energy, however, our geometric-mean results are virtually identical with those of Fielder and Armstrong[6] and of Brown, Carter, and Kelly.[4] These other calculations include excitations out of the $3s$ subshell; ours do not.

Generalization of our OSTM method to treat the $3s$ and $3p$ subshells simultaneously, rather than only the $3p$ subshell, appears warranted to reduce the remaining difference between our length and velocity cross-section results to values comparable to those obtained by calculations that do treat both subshells simultaneously. Our geometric-mean cross sections, however, are not expected to change significantly except possibly at the ^1S threshold.

ACKNOWLEDGMENTS

This work was supported in part by National Science Foundation Grant No. PHY-80-26055 at the University of Nebraska and by National Science Foundation Grant No. PHY-80-09146 at the University of Southern California.

[1](a) M. J. Conneely, Ph.D. thesis, London University, 1969 (unpublished); (b) M. J. Conneely, K. Smith, and L. Lipsky, J. Phys. B **3**, 493 (1970).

[2]A. F. Starace and L. Armstrong, Jr., Phys. Rev. A **13**, 1850 (1976).

[3]N. A. Cherepkov and L. V. Chernysheva, (a) Phys. Lett. **60A**, 103 (1977); (b) Izv. Akad. Nauk SSSR, Ser. Fiz. **41**, 2518 (1977) [Bull. Acad. Sci. USSR, Phys. Ser. **41**, 47 (1977)].

[4]E. R. Brown, S. L. Carter, and H. P. Kelly, (a) Phys. Lett. **66A**, 290 (1978); (b) Phys. Rev. A **21**, 1237 (1980).

[5]M. Lamoureux and F. Combet Farnoux, J. Phys. (Paris) **40**, 545 (1979).

[6](a) W. R. Fielder and L. Armstrong, Jr., Phys. Rev. A **28**, 218 (1983); (b) William Reynolds Fielder, Ph.D. thesis, Johns Hopkins University, 1981 (available through University Microfilms International, 300 N. Zeeb Road, Ann Arbor, Michigan 48106, Order No. 8106608).

[7]A. F. Starace, *Theory of Atomic Photoionization,* in *Handbuch der Physik,* edited by W. Mehlhorn (Springer, Berlin, 1982), Vol. 31, pp. 1—121. See especially Chap. III and references therein.

[8]B. Ruščić and J. Berkowitz, Phys. Rev. Lett. **50**, 675 (1983).

[9]K. Kimura, T. Yamazaki, and Y. Achiba, Chem. Phys. Lett. **58**, 104 (1978).

[10]A. F. Starace and S. Shahabi, Phys. Rev. A **25**, 2135 (1982).

[11]T. N. Chang and U. Fano, Phys. Rev. A **13**, 263 (1976); **13**, 282 (1976).

[12]Siamak Shahabi, Ph.D. thesis, The University of Nebraska, 1983 (available through University Microfilms International, 300 N. Zeeb Road, Ann Arbor, Michigan 48106, Order No. DA8328194).

[13]M. Ya. Amusia and N. A. Cherepkov, Case Stud. At. Phys. **5**, 47 (1975).

[14]L. Armstrong, Jr., J. Phys. B **7**, 2320 (1974).

[15]D. J. Rowe and C. Ngo-Trong, Rev. Mod. Phys. **47**, 471 (1975).

[16]E. Dalgaard, J. Phys. B **8**, 695 (1975).

[17]A. F. Starace, in *Physics of Electronic and Atomic Collisions,* edited by S. Datz (North-Holland, Amsterdam, 1982), pp. 431—446.

[18]K. Smith, R. J. W. Henry, and P. G. Burke, Phys. Rev. **147**, 21 (1966).

[19]See A. F. Starace, Ref. 7, p. 73 and references therein.

[20]R. J. W. Henry and L. Lipsky, Phys. Rev. **153**, 51 (1967).

[21]L. S. Rodberg and R. M. Thaler, *Introduction to the Quantum Theory of Scattering* (Academic, New York, 1967), Chap. 9.

[22]A. F. Starace, Ref. 7, pp. 15—23.

[23]P. de A. P. Martins, J. Phys. B **1**, 154 (1968); Proc. Cambridge Philos. Soc. **69**, 167 (1971).

[24]A. F. Starace, Ref. 7, pp. 8—15.

[25]R. T. Pu and E. S. Chang, Phys. Rev. **151**, 31 (1966).

[26]H. J. Silverstone and M. L. Yin, J. Chem. Phys. **49**, 2026 (1968).

[27]S. Huzinaga and C. Arnau, Phys. Rev. A **1**, 1285 (1970).

[28]T. N. Chang, Phys. Rev. A **16**, 1171 (1977).

[29]T. N. Chang, Phys. Rev. A **18**, 1448 (1978).

[30]T. N. Chang and R. T. Poe, J. Comput. Phys. **12**, 557 (1973).

[31]C. E. Moore, *Ionization Potentials and Ionization Limits Derived from the Analyses of Optical Spectra* (U.S. GPO, Washington, D.C., 1970).

[32]G. N. Bates, Comput. Phys. Commun. **8**, 220 (1974).

[33]A. F. Starace, Ref. 7, pp. 38 and 39.

[34]A. F. Starace, Ref. 7, Eq. (6.6a).

[35]A. E. Hansen, Mol. Phys. **13**, 425 (1967).

[36]A. F. Starace, Phys. Rev. A **2**, 118 (1970).

[37]L. Lipsky and J. Cooper (unpublished); length and velocity results presented in Fig. 1 of Ref. 36.

[38]J. A. R. Samson, Adv. At. Mol. Phys. **2**, 178 (1966).

[39]T. N. Chang, Phys. Rev. A **15**, 2392 (1977).

[40]J. A. R. Samson and J. L. Gardner, J. Opt. Soc. Am. **62**, 856 (1972), Eq. (5).